Inorg. Chem. **2007**, *46*, 6148–6154

Hybrid Perovskite Resulting from the Solid-State Reaction between the Organic Cations and Perovskite Layers of α1-(Br-$(CH_2)_2$-$NH_3)_2PbI_4$

Sebastien Sourisseau,[†] Nicolas Louvain,[†] Wenhua Bi,[†] Nicolas Mercier,*[,†] David Rondeau,[†] Jean-Yves Buzaré,[‡] and Christophe Legein[‡]

Laboratoire de Chimie, Ingénierie Moléculaire et Matériaux d'Angers, UMR-CNRS 6200, Université d'Angers, 2 Bd Lavoisier, 49045 Angers, France, Laboratoire des Oxydes et Fluorures, CNRS UMR 6010 and Laboratoire de Physique de l'Etat Condensé, CNRS UMR 6087, Institut de Recherche en Ingénierie Moléculaire et Matériaux Fonctionnels, CNRS FR 2575, Université du Maine, Avenue Olivier Messiaen, 72085 Le Mans Cedex 9, France

Received February 7, 2007

The α1-(Br-$(CH_2)_2$-$NH_3)_2PbI_4$ hybrid perovskite undergoes a solid-state transformation, that is, the reaction between the organic cations and the perovskite layers to give the new hybrid perovskite (Br-$(CH_2)_2$-$NH_3)_{2-x}$(I-$(CH_2)_2$-$NH_3)_x$-$PbBr_xI_{4-x}$, based on mixed halide inorganic layers. This transformation has been followed by a conventional powder X-ray diffraction system equipped with a super speed detector, and both solid-state ^{13}C NMR and ESI/MS measurements have been adopted in the estimation of the rate of halide substitution. The first reaction step leads to the special composition of $x \approx 1$ (A phase), while the complete substitution is not achieved even at elevated temperature ($x_{max} \approx 1.85$ (B phase)). This unprecedented solid-state reaction between organic and inorganic components of a hybrid perovskite can be considered as a completely new strategy to achieve interesting hybrid perovskites.

Introduction

Organic−inorganic hybrids are of great interest and importance for many applications not only because of the ability to combine peculiar properties of both components but also because of the potential to tune functions through slight structural modifications at the organic−inorganic interface. Hybrid perovskites with semiconducting properties, which have the great advantage of being processed into thin films by room-temperature techniques such as spin-coating,[1] can be applied to channel materials in thin-film field-effect transistors (TFTs).[2,3] For instance, the charge carrier mobility in $(C_6H_5C_2H_4NH_3)_2SnI_4$[2] is 0.6 $cm^2\ V^{-1}\ s^{-1}$. Two feasible strategies have been considered to improve the charge carrier mobility of a given halogenometalate network: (1) to enhance the dimensionality of the structure to either multilayers[4] or monolayers bridged by covalent bond[5] and (2) to tune the band gap associated to perovskite layers by adopting selected cations, which are able to change the structure of the inorganic framework.[6,7] Recently, we prepared new hybrids based on X-$(CH_2)_2$-NH_3^+ (X = Br, Cl) cations with reduced band gap.[7]

At present, a new approach based on the decomposition of highly soluble hybrid precursors at low temperature (about 200 °C) to produce spin-coated thin films of semiconducting materials has also been demonstrated. Continuous crystalline chalcogenide semiconducting films were prepared by such a two-step process. It is remarkable that those films exhibit an n-type transport with a mobility of more than 10 $cm^2\ V^{-1}$

* To whom correspondence should be addressed. Fax: 33.(2).41.73.54.05. Phone: 33.(2).41.73.50.83. E-mail: nicolas.mercier@univ-angers.fr.
† Université d'Angers.
‡ Université du Maine.

(1) (a) Mitzi, D. B. *Chem. Mater.* **2001**, *13*, 3283. (b) Mitzi, D. B. *J. Mater. Chem.* **2004**, *15*, 2355.
(2) Kagan, C. R.; Mitzi, D. B.; Chondroudis, K. *Science* **1999**, *286*, 945.
(3) Mitzi, D. B.; Chondroudis, K.; Kagan, C. R. *IBM. J. Res. Dev.* **2001**, *45*, 1.
(4) (a) Calabrese, J.; Jones, N. L.; Harlow, R. L.; Herron, N.; Thorn, D. L.; Wang, Y. *J. Am. Chem. Soc.* **1991**, *113*, 2328. (b) Mitzi, D. B.; Feild, C. A.; Harrison, W. T.; Guloy, A. M. *Nature* **1994**, *369*, 467. (c) Zhu, X. H.; Mercier, N.; Riou, A.; Blanchard, P.; Frère, P. *Chem. Commun.* **2002**, *18*, 2160.
(5) Mercier, N.; Riou, A. *Chem. Commun.* **2004**, *7*, 844.
(6) (a) Xu, Z.; Mitzi, D. B.; Dimitrakopoulos, C. D.; Maxcy, K. R. *Inorg. Chem.* **2003**, *42*, 2031. (b) Mitzi, D. B.; Dimitrakopoulos, C. D.; Kosbar, L. L. *Chem. Mater.* **2001**, *13*, 3728. (c) Xu, Z.; Mitzi, D. B.; Medeiros, D. R. *Inorg. Chem.* **2003**, *42*, 1400. (d) Mercier, N.; Poiroux, S.; Riou, A.; Batail, P. *Inorg. Chem.* **2004**, *43*, 8361.
(7) Sourisseau, S.; Louvain, N.; Bi, W.; Mercier, N.; Rondeau, D.; Boucher, F.; Buzaré, J. Y.; Legein, C. *Chem. Mater.* **2007**, *19*, 600.

10.1021/ic070240g CCC: $37.00
Published on Web 06/27/2007

s^{-1}.[8] In the field of hybrid perovskites, another kind of a two-step process has been reported in several compounds based on polymerizable monomer cations: first of all, the perovskite compound was synthesized by using corresponding molecular entities; then photochemical polymerization reactions between the organic ligands take place, and polymers such as polybutadiene,[9] polyacetylene,[10] polythiophene[11] were formed in the solid state. However, those polymerization reactions have no effect on the structural and electronic properties of perovskite layers. To our knowledge, there was no report about the reaction between the organic and inorganic parts of these layered compounds so far. Herein, we report the unprecedented organic−inorganic solid-state reaction which takes place in α1-(Br-$(CH_2)_2$-$NH_3)_2PbI_4$ and the resultant mixed halide perovskite of (Br-$(CH_2)_2$-$NH_3)_{2-x}$(I-$(CH_2)_2$-$NH_3)_xPbBr_xI_{4-x}$ (with $x_{max} = 1.85$).

Experimental Section

X-ray Crystallography. Powder X-ray diffraction measurements were carried out on a D8 Brucker diffractometer using Cu $K\alpha_{1,2}$ radiation, equipped with the linear Vantec super speed detector and with a TTK450 temperature chamber. During the phase transformation study, 15 min diffractograms were collected in the range of 6−40°. Cell determinations were performed using the DICVOL program,[12] cell parameters refinements being carried out using the profile-fitting program of TOPAS[13] (ESI).

Solid-State NMR. Cross polarization (CP) combined with magic angle spinning (MAS) solid-state $^1H-^{13}C$ NMR experiments were carried out at room temperature on a Bruker Avance 300 wide bore spectrometer at 75.47 Mhz. A 2.5 mm CPMAS probe was used at spinning frequency equal to 10 kHz. ^{13}C isotropic chemical shifts (δ_{iso}) are expressed in ppm using TMS as external reference. The ^1H radiofrequency (rf) was set to obtain $\tau_{\pi/2} = 4$ μs. The contact time was taken equal to 0.8 ms. 16 k transients were accumulated. The recycle delay was 1 s. The reconstructions of the spectra (SI) were performed with DMFIT[14] software. Recent experiments[7] on the starting material α1/α2-(Br-$(CH_2)_2$-$NH_3)_2PbI_4$ and on (Br-$(CH_2)_2$-NH_3)Br and (I-$(CH_2)_2$-$NH_3)_2PbI_4$ salts (see SI) have shown that, under these acquisition conditions, the CPMAS technique is quantitative.

Mass Spectrometry. MS analyses were performed on a JMS-700 double-focusing mass spectrometer with reversed geometry (JEOL, Akishima, Tokyo, Japan), equipped with a pneumatically assisted ESI source. Nitrogen was used as the nebulizer gas. The positive ion mode was used with the needle voltage adjusted to obtain an ∼100 nA needle current, that is, typically ∼3 kV. The desolvating plate and orifice 1 temperatures were set to 130 and 85 °C, respectively. The sample was introduced into the ESI interface via a PHD 2000 infusion syringe pump (Harvard Apparatus, Holliston, MA) at a 30 μL min^{-1} flow rate. A 5 kV acceleration voltage was applied. The low-resolution full-scan mass spectra (typically $R = 1500$ at 10% valley) were obtained by scanning the magnetic field over a wide range of mass-to-charge ratios. The PEGs used for calibration have nominal molecular masses centered around 400, 1500, and 2000. For the measurement of relative intensities, the ion peak intensity values were calculated by averaging the signals measured on each set of ten scans. Note that in the case of relative intensity measurements in the low mass-to-charge ratio range, the orifice 1 voltage value was increased until no signal appears beyond 300 Th. MS^n analyses were performed on a Finnigan LCQ Classic ion trap mass spectrometer (Thermo Electron Corporation, San Jose, CA). The entire isotopic envelope of the ion *m*/*z* 1089 was isolated (center of mass *m*/*z* 1089 and isolation window of *m*/*z* 10), activated and dissociated in conditions that were optimized such that the precursor ions mainly yielded the mass *m*/*z* 376 ion upon dissociation. The entire distribution of the latter was isolated in the ion trap (center mass *m*/*z* 376 and isolation window of *m*/*z* 6). Dissociation of the selected precursor ions was subsequently achieved through collisional activation using helium buffer gas as the collision partner. The MS^3 experiments were then completed by isolation, activation, and dissociation of the entire distribution of the *m*/*z* 376 product ion.

Results and Discussion

The recently obtained polymorph compounds α1-(Br-$(CH_2)_2$-$NH_3)_2PbI_4$ and α2-(Br-$(CH_2)_2$-$NH_3)_2PbI_4$ crystallize in a monoclinic cell (*C*2/c, $a = 9.126(1)$ Å, $b = 9.143(1)$ Å, $c = 21.450(2)$ Å, $\beta = 98.65(1)°$, $V = 1769.4(3)$ $Å^3$) and an orthorhombic cell (Pbnm, $a = 6.4824(3)$ Å, $b = 12.9046(8)$ Å, $c = 21.141(2)$ Å, $V = 1768.5(2)$ $Å^3$), respectively.[7] Both layered structures are built up from undistorted PbI_4 perovskite layers which were separated by ammonium cations. The distances between layers are 10.72 and 10.57 Å, respectively, and are approximately equal to half of the length of *c* axis (Figure 1a, α1-phase). DSC measurements of a sample containing a mixture of α1-(Br-$(CH_2)_2$-$NH_3)_2PbI_4$ (main phase) and α2-(Br-$(CH_2)_2$-$NH_3)_2PbI_4$ reveals two endothermic peaks at $T = 107$ and 153 °C, which were much lower than the temperature of decomposition ($T = 225$ °C, TGA, see SI). When the samples were heated on a Köfler apparatus, the change in color corresponded with the thermal accidents: first, the color changed from red to orange and then from orange to yellow. Moreover, we noticed that the heated samples retain their color when they were cooled to room temperature. The irreversibility of these transitions has been confirmed by the absence of peak on the DSC curves (20−200 °C range) of a sample previously heated at 160 °C, and during the cooling step of a sample previously heated at 120 °C (SI). We also observed that crystals heated a long time at relatively low temperature (50−70 °C range) were transformed into orange crystals. The thermochromism phenomenon has already been described in such compounds as the result of structural changes of the perovskite layers.[6d,15] In contrast, we are going to show that the nature of the

(8) (a) Mitzi, D. B.; Kosbar, L. L.; Murray, C. E.; Coppel, M.; Afzali, A. *Nature* **2004**, *428*, 299.
(9) (a) Tieke, B.; Wegner, G. *Angew. Chem., Int. Ed.* **1981**, *20*, 687. (b) Tieke, B.; Chapuis, G. *Mol. Cryst. Liq. Cryst.* **1986**, *137*, 101.
(10) (a) Takeoka, Y.; Asai, K.; Rikukawa, M.; Sanui, K. *Chem. Commun.* **2001**, 2592. (b) Kosuge, H.; Okada, S.; Oikawa, H.; Nakanishi, H. *Mol. Cryst. Liq. Cryst.* **2002**, *377*, 13.
(11) (a) Era, M. *Chem. Lett.* **2003**, *3*, 272. (b) Era, M.; Yoneda, S.; Sano, T.; Noto, M. *Thin Film Solid* **2003**, *438*, 322.
(12) DICVOL04: Boultif, A.; Louer, D. *J. Appl. Crystallogr.* **2004**, *37*, 724−731.
(13) *TOPAS*, 2.1 version, Bruker AXS; Madison WI.
(14) Massiot, D.; Fayon, F.; Capron, M.; King, I.; Le, Calvé, S.; Alonso, B.; Durand, J.-O.; Bujoli, B.; Gan, Z.; Hoatson, G. *Magn. Reson. Chem.* **2002**, *40*, 70−76.
(15) (a) Willet, R. D.; Hangen, J. A.; Lebsack, J.; Money, J. *Inorg. Chem.* **1974**, *13*, 2510. (b) Ishihara, T.; Takahashi, J.; Goto, T. *Solid State Commun.* **1989**, *69*, 933.

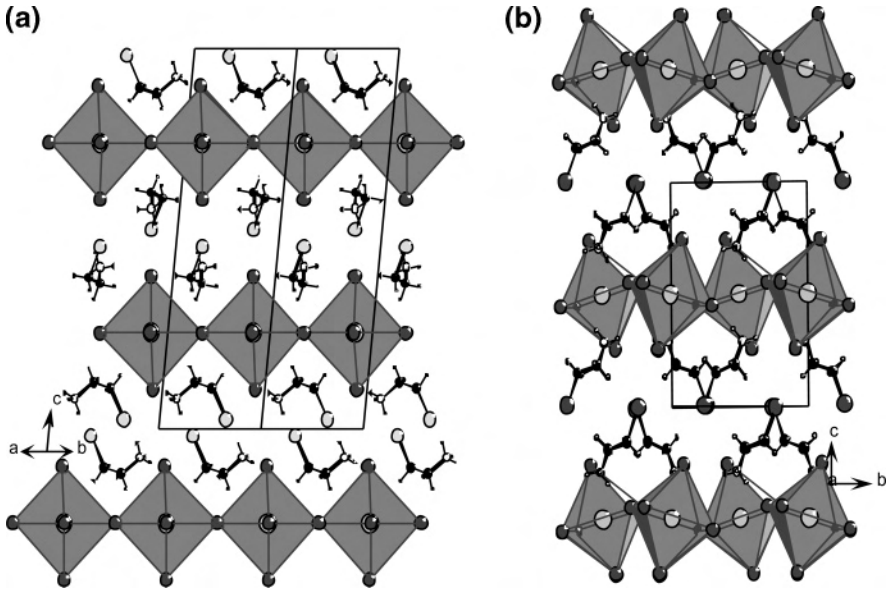

Figure 1. View of the layered hybrid perovskite structures of α1-(Br-$(CH_2)_2$-$NH_3)_2PbI_4$ (a) and (I-$(CH_2)_2$-$NH_3)_2PbI_4$ (b).

transformation in our research work is a reaction in the solid state consisting of a halide substitution of organic bromine by iodide belonging to the inorganic framework. The heating (50 °C, 40 h) of red crystals of α1-(Br-$(CH_2)_2$-$NH_3)_2PbI_4$ involves it bursting into many fragments of orange crystals. We tentatively performed the crystal structure determination of the resulting new phase. The overall atomic arrangement of the monoclinic structure ($P2_1/n$, $a = 8.524(8)$ Å, $b = 8.685(1)$ Å, $c = 25.583(5)$ Å, $\beta = 99.71(1)°$, $V = 1845(1)$ Å^3) consists of PbX_4 perovskite layers separated by molecules that stand in the interlayer space, their ammonium part being located in the perovskite sheets. This situation which differs from that of α1-(Br-$(CH_2)_2$-$NH_3)_2PbI_4$ can be compared to that recently observed in the structure of (I-$(CH_2)_2$-$NH_3)_2$-PbI_4 ($P2_1$/a, $a = 8.753(1)$ Å, $b = 8.747(1)$ Å, $c = 12.720(2)$ Å, $\beta = 97.63(1)°$, $V = 965.3(2)$ Å^3),[7] given in Figure 1b. Nevertheless, because of the poor data quality, we could not define the nature of halide belonging both to perovskite layers and cations in this structure (crystal data given as SI).

Because of the relatively low speed of the solid-state reaction under mild conditions, the reaction could be followed by using a conventional powder X-ray diffractometer equipped with a fast speed detector, and it was estimated that a data collection of 15 min was long enough to get patterns in quite good quality On the other hand, it was short enough to consider that there was no strong structural change. Thus, 15 min diffractograms in the 6−40° 2θ range were collected every 30 min, first at 50 °C during 72 h, then 65 h at 80 °C, and finally at 110, 130, and 150 °C (Figure 2). At 50 °C, it is easy to notice the disappearance of the peak at 14.3° within 20 h, which corresponds to the phase transformation from α2-(Br-$(CH_2)_2$-$NH_3)_2PbI_4$ to α1-(Br-$(CH_2)_2$-$NH_3)_2PbI_4$, because the peak at 14.3° is the unique diffraction of α2-(Br-$(CH_2)_2$-$NH_3)_2$ PbI_4. The main reaction starts as underlined by the graduated disappearance of the (002) line of α1-(Br-$(CH_2)_2$-$NH_3)_2PbI_4$ (8.4° 2θ). At the same time, a new line grows at lower angle of 7.9° 2θ and rapidly fades, while a lower angle peak at

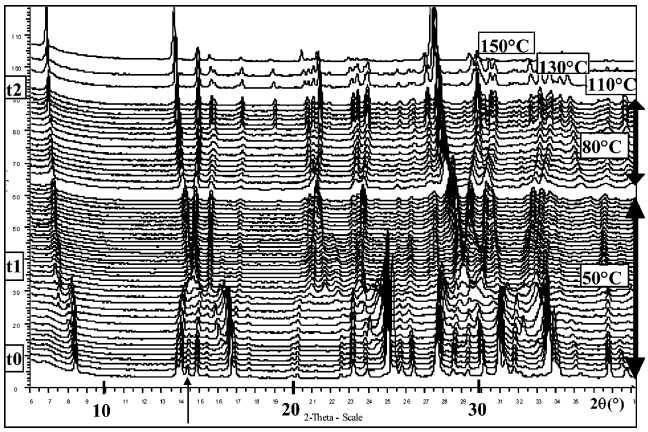

Figure 2. Solid-state transformation followed by X-ray powder thermodiffractometry. XRPD patterns collected in the range of 50−150 °C (arrow, line at 14.3°).

7.5° 2θ appears. These two lines are probably the (002) lines of intermediate phases. Finally, after it was heated at 50 °C for 24 h (Figure 2, t1), the initial phase is transformed completely into a new phase **A** characterized by its low angle peak of 7.3° 2θ. It is obvious that the change indicates a prolonged *c*-axis, that is, the distance between the perovskite layers is increased. The powder pattern of **A** has been indexed in the monoclinic cell $a = 8.672(1)$ Å, $b = 8.760(1)$ Å, $c = 25.382(3)$ Å, $\beta = 99.16(1)°$, which is in good agreement with the single-crystal unit cell determination previously mentioned. Then, as indicated by the evolution of the 2θ positions of lines in the XRPD patterns, the transformation is still going on at 50 °C and at higher temperature. It is necessary to point out that all X-ray patterns collected up to 150 °C can also be indexed in the same monoclinic unit cell, which notably indicates that there is no decomposition during the process. We can notice that the evolution of cell parameters, that is, a decrease of *a* and *b* and an increase of *c*, is quite regular from $t = 24$ (t1) to 137 h (t2) (Figure 3). At higher temperature ($T = 110$ °C,

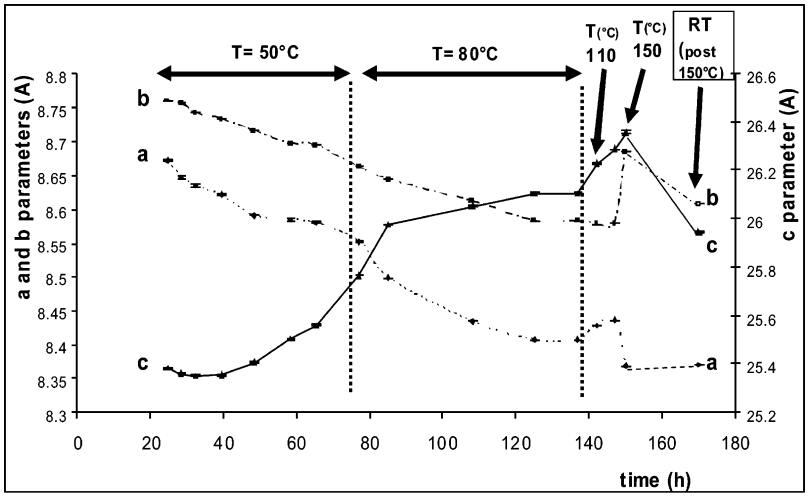

Figure 3. Evolution of the *a*, *b*, *c* monoclinic cell parameters of a sample of α1-/α2-(Br-$(CH_2)_2$-$NH_3)_2PbI_4$ previously heated at 50 °C for 24 h (**A** phase, (Br-$(CH_2)_2$-$NH_3)_{2-x}$(I-$(CH_2)_2$-$NH_3)_x$$PbBr_xI_{4-x}$ ($x \approx 1$)).

Table 1. Relative Intensities and Nature of Ions Observed in the Full Scan ESI Mass Spectra of Samples of α1-/α2-(Br-$(CH_2)_2$-$NH_3)_2PbI_4$ Previously Heated at 50 °C during 24 h (**A** Phase) and Heated at 150 °C (**B** Phase)

Ion	m/z value of the monoisotopic peak	Relative Intensity (**A**)	Relative Intensity (**B**)
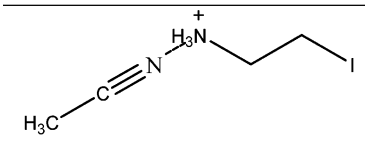	213	22.41	32
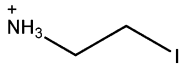	172	15.39	23.97
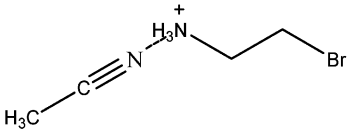	165	19.22	2.17
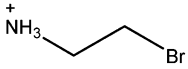	124	17.75	1.77

130 °C), the *c* and *a* parameters increase monotonously, which is opposite to *b*. Finally, a temperature as high as 150 °C is necessary to pass through a last reaction step as indicated by the abrupt change of *a* and *b* (see Figure 3), this feature being correlated to the change of color of the sample already mentioned, from orange to yellow. The room-temperature cell parameters of the sample previously heated at 150 °C (**B** phase) have been refined as $a = 8.3707(2)$ Å, $b = 8.6066(2)$ Å, $c = 25.9462(3)$ Å, $\beta = 98.54(1)°$ (reported in Figure 3).

The nature of the solid-state reaction was unambiguously proved by MS^n analysis and CPMAS solid-state $^1H-^{13}C$ NMR spectroscopy, which both allow to measure Br-$(CH_2)_2$-NH_3^+ and I-$(CH_2)_2NH_3^+$ cations quantitatively.

The electrospray mass spectrum (ESI/MS) of the starting product α1-/α2-(Br-$(CH_2)_2$-$NH_3)_2PbI_4$ exhibits an isotopic pattern observed in the mass to charge (*m*/*z*) ratio centered on the *m*/*z* 1089 peak. This signal is assigned to the [(Br-$(CH_2)_2$-$NH_3)_3PbI_4]^+$ monocharged species. The nature of the organic and inorganic moieties of the later is confirmed by MS^3 experiments. After selection and fragmentation of the *m*/*z* 1089 parent ion, the *m*/*z* 376 daughter ion [(Br-$(CH_2)_2$-$NH_3)_2I]^+$ undergoes, in turn, collision-induced dissociation (CID) for leading to the formation of charged species whose monoisotopic peak is detected at the *m*/*z* 124, *m*/*z* 165 (Table 1, Figure 4), and *m*/*z* 246 values. The results of the MS^3 experiment indicate that the *m*/*z* 1089 ion is characteristic of the starting product structure since only cations characteristic to the organic phase Br$(CH_2)_2NH_3^+$ are detected after the decay of the [(Br-$(CH_2)_2$-$NH_3)_3PbI_4]^+$ monocharged species. Note that the formation of the *m*/*z* 165 ion is not astonishing since several works have shown that the addition reactions of molecule such as acetonitrile on electrosprayed cations can occur from residual solvent vapor in the plume of the electrospray emitter or further downstream of the mass spectrometer.[16] Such behavior is often observed, namely, in

(16) (a) Gabelica, V.; Lemaire, D.; Laprévote, O.; De Pauw, E. *Int. J. Mass Spectrom.* **2001**, *210/211*, 113. (b) Schlosser, G.; Takats, Z.; Vékey, K. *J. Mass Spectrom.* **2003,** *38*, 1245. (c) Rondeau, D.; Perruchas, S.; Avarvari, N.; Batail, P.; Vékey, K. *J. Mass Spectrom.* **2005**, *40*, 60.

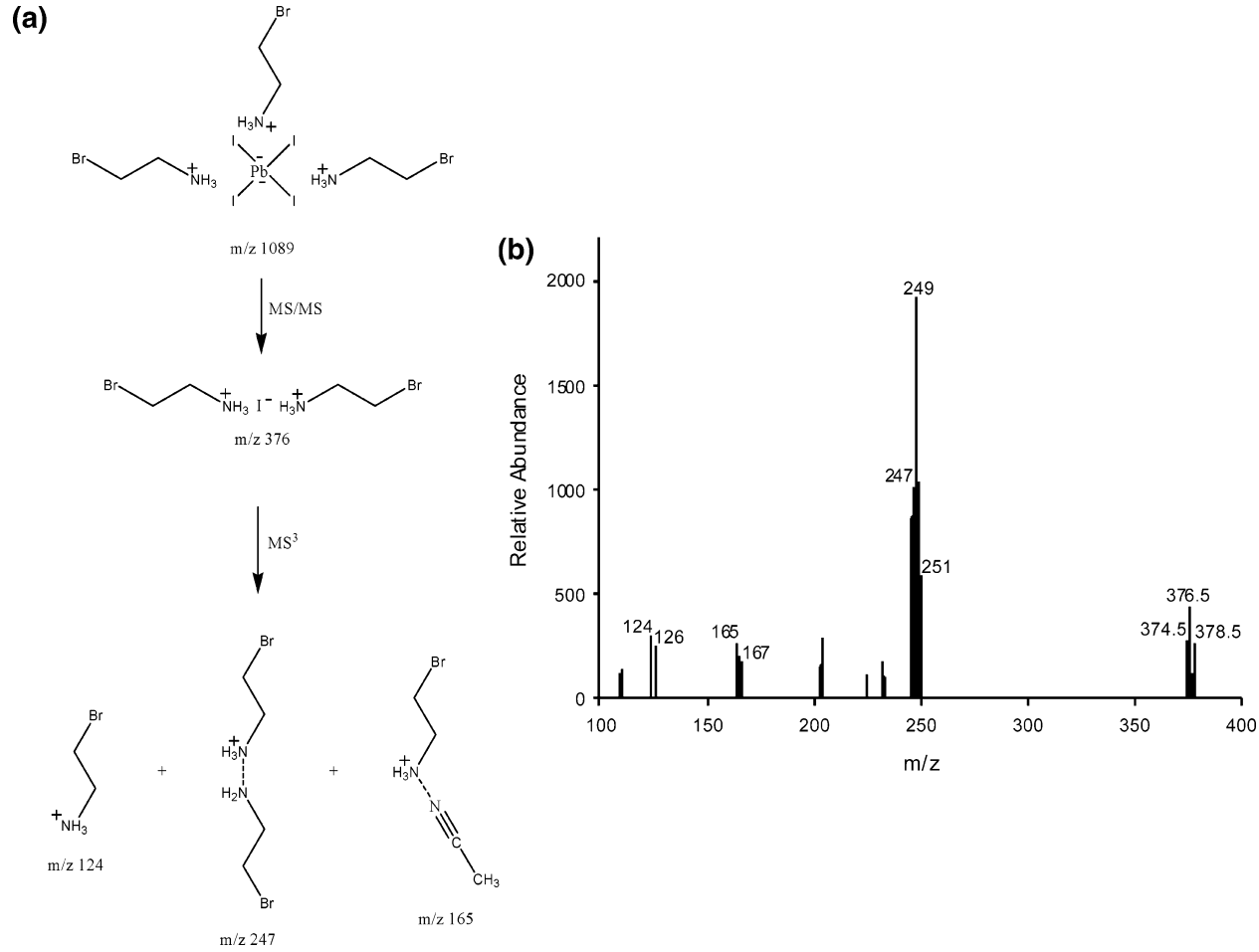

Figure 4. Structures of the ions (**a**) produced from positive ion ESI-MS^3 mass spectrum of *m*/*z* 376 ion from the *m*/*z* 1089 ion (1089 > 376) (**b**).

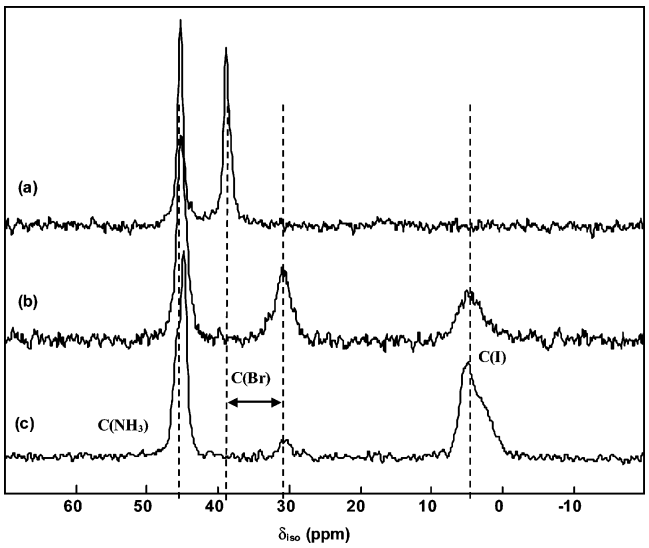

Figure 5. CPMAS solid state $^1H-^{13}C$ NMR spectra of α1-/α2-(Br-$(CH_2)_2$-$NH_3)_2PbI_4$ (a), α1-/α2-(Br-$(CH_2)_2$-$NH_3)_2PbI_4$ heated 24 h at 50 °C (**A** phase) (b), and α1-/α2-(Br-$(CH_2)_2$-$NH_3)_2PbI_4$ heated at 150 °C (**B** phase) (c).

the case of the use of magnetic or ion trap mass spectrometer. Behind the structural identification, it must be noted that the structure of the *m*/*z* 376 ion directly produced from the *m*/*z* 1089 (Figure 4) is in agreement with the interactions at the organic−inorganic interface highlighted for α1- or α2-(Br-$(CH_2)_2$-$NH_3)_2PbI_4$.[7] The latter involves the hydrogen bonding

Table 2. Isotropic Chemical Shifts, δ_{iso} (ppm) and Relative Intensities (%) as Deduced from Spectrum Reconstruction (SI) and Line Assignments for α1-/α2-(Br-$(CH_2)_2$-$NH_3)_2PbI_4$ and for Samples of α1-/α2-(Br-$(CH_2)_2$-$NH_3)_2PbI_4$ Previously Heated at 50 °C during 24 h (**A** Phase) and Heated at 150 °C (**B** Phase)

sample	δ_{iso}	relative intensity	line assignment
α1-/α2-(Br-$(CH_2)_2$-$NH_3)_2PbI_4$	38.9	50.0	C(Br)
	45.4	50.0	C(NH_3)
A phase	4.5	26.0	C(I)
	30.9	25.5	C(Br)
	45.2	48.5	C(NH_3)
B phase	∼4	46.9	C(I)
	30.6	4.3	C(Br)
	∼45	48.8	C(NH_3)

of the ammonium and halogen of the terminal bromide of the organic moiety with the apical iodides of the PbI_4 layer. It could be also interesting to relate the formation of the *m*/*z* 247 ion with the degradation of the starting materials by HI emission. For the **A** and **B** samples, the ESI full scan mass spectra exhibit characteristic signals whose structures and *m*/*z* values are reported in Table 1, together with corresponding intensities. From the results, it appears that the solid-state reaction can be evidenced by monitoring the appearance of the cations Br-$(CH_2)_2$-NH_3^+ and I-$(CH_2)_2$-NH_3^+, which are specific of the starting product and the reaction product, respectively. Indeed, according to the literature, it is possible to correlate the relative intensities of these ions reported in Table 1 with the relative amount of the charge organic

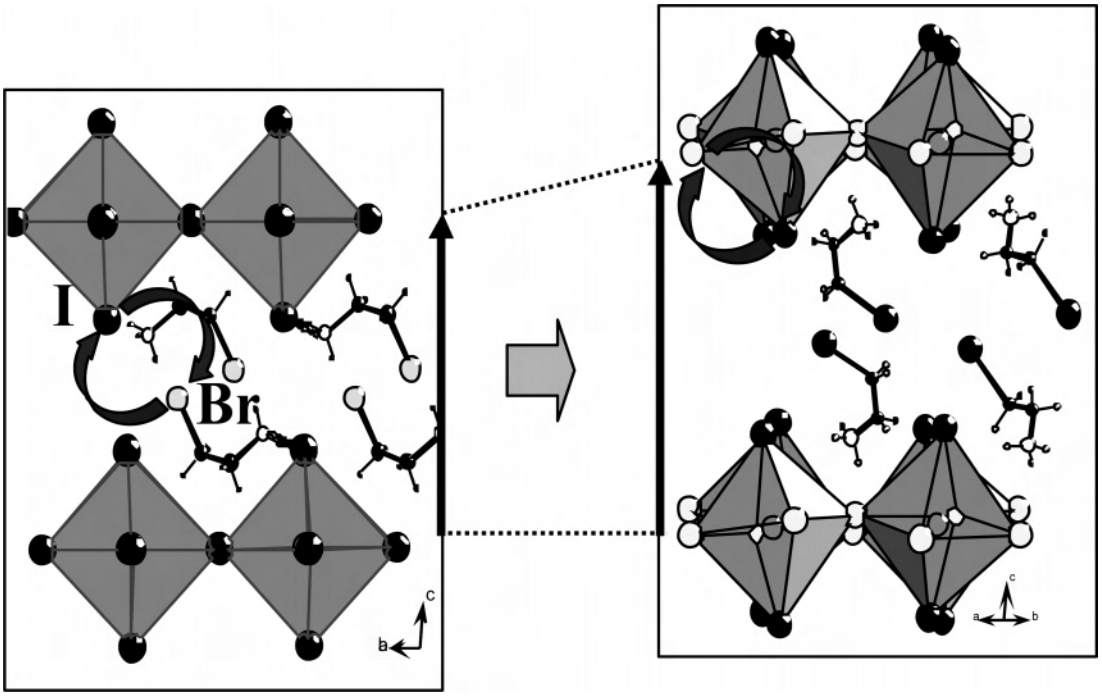

Figure 6. Hypothetical mechanism of the solid-state reaction: From α1-(Br-$(CH_2)_2$-$NH_3)_2PbI_4$ to (I-$(CH_2)_2$-$NH_3)_2PbBr_2I_2$.

species present in the electrosprayed solutions.[17] The ESI/MS analyses of these two cations allow to take in account in a first approximation a same ionization efficiency. Moreover, a same gas-phase ion sensitivity coefficient is expected since during the transfer process into the gas-phase, one can assume that the cations $Br(CH_2)_2NH_3^+$ and $I(CH_2)_2NH_3^+$ have the same surface activity when they leave the droplets to become gas-phase ions.[17] One can then consider that the initial sample heated 24 h at 50 °C (**A** phase) contains 50.5 and 49.5% of Br-$(CH_2)_2$-NH_3^+ and I-$(CH_2)_2$-NH_3^+ cations, respectively. For the sample heated at 150 °C (**B** phase), the ratio is 6.6/93.4%.

CPMAS $^1H-^{13}C$ solid-state NMR experiments were all carried out at room temperature. Experiments on the starting material α1-/α2-(Br-$(CH_2)_2$-$NH_3)_2PbI_4$ (Figure 5a, Table 2) and on (Br-$(CH_2)_2$-NH_3)Br and (I-$(CH_2)_2$-$NH_3)_2PbI_4$ salts (SI) were carried out recently[7] allowing the determination of the isotropic chemical shift values of the C(X) and C(NH_3) atoms for both $X(CH_2)_2NH_3^+$ (X = Br, I) cations: δ_{iso} C(NH_3) ≈ 45 ppm, δ_{iso} C(I) ≈ 4 ppm, δ_{iso} C(Br) ≈ 31 ppm in (Br-$(CH_2)_2$-NH_3)Br and δ_{iso} C(Br) ≈ 39 ppm in α1-/α2-(Br-$(CH_2)_2$-$NH_3)_2PbI_4$. The unusual situation of Br-$(CH_2)_2$-NH_3^+ cations in the crystal structures of α1- and α2-(Br-$(CH_2)_2$-$NH_3)_2PbI_4$ induces this higher later value compared to the one in (Br-$(CH_2)_2$-NH_3)Br.[7] The spectrum of the initial sample heated 24 h at 50 °C (**A** phase, Figure 5b) displays three peaks at 45, 31, and 4 ppm that can be assigned to C(NH_3) atoms, C(Br) atoms, and C(I) atoms, respectively. This result testifies the presence of both $I(CH_2)_2NH_3^+$ and $Br(CH_2)_2NH_3^+$ cations in the sample and, as a consequence, unambiguously demonstrates that a solid-state reaction has occurred between molecules and perovskite layer components. As from the analysis of MS, a 1:1 ratio of the two different cations (Table 2) has been estimated from spectrum reconstruction (SI), leading to the formula of (Br-$(CH_2)_2$-NH_3)(I-$(CH_2)_2$-NH_3)$PbBrI_3$. The latter corresponding to the **A** phase can be more rightly considered as the $x \approx 1$ term of the solid solution (Br-$(CH_2)_2$-$NH_3)_{2-x}$(I-$(CH_2)_2$-$NH_3)_x$-$PbBr_xI_{4-x}$. Note that the discrepancy between ^{13}C isotropic chemical shifts in α1- or α2-(Br-$(CH_2)_2$-$NH_3)_2PbI_4$ (39 ppm) and in (Br-$(CH_2)_2$-$NH_3)_{2-x}$(I-$(CH_2)_2$-$NH_3)_xPbBr_xI_{4-x}$ ($x \approx 1$) (31 ppm) for C(Br) atoms clearly indicates two different situations for Br-$(CH_2)_2$-NH_3^+ cations in structures. The relative intensities of the peaks at 4 and 31 ppm are changing along with the experiment ($t > t_1 = 24$ h), which indicates the halide substitution reaction is still going on (increasing x). At this point, we can note that the first reaction step can be related to the ideal structure of α1-(Br-$(CH_2)_2$-$NH_3)_2PbI_4$ for an exchange reaction between both components due to the close proximity of the apical I and the C atom bearing Br (Figure 1). On the other hand, it is somewhat more difficult to understand the reasons why the exchange reaction is going on since molecules stand up between layers after the first reaction step. Finally, the equilibrium of the substitution reaction between organic bromine and iodine atoms was achieved and cannot be moved even at 150 °C (Figure 5c). It results in the formation of the new compound (**B** phase), (Br-$(CH_2)_2$-$NH_3)_{2-x}$(I-$(CH_2)_2$-$NH_3)_xPbBr_xI_{4-x}$ with $x \approx 1.85$, the ratios of I-$(CH_2)_2$-NH_3^+ to Br-$(CH_2)_2$-NH_3^+ being 92:8 and 93.4:6.6 according to the NMR and MS, respectively.

Several hybrids based on mixed halide perovskite layers $M^{II}(X_{1-x}X_x')_4$ (M = Pb, Cu, Cr; X, X′ = I, Br, Cl) have

(17) Kebarle, P. *J. Mass Spectrom.* **2000**, *35*, 804 and references cited therein.

been reported so far.[18] In particular, the influence of the X/X′ ratio on the optical properties has been investigated.[18a,b] In their article dealing with crystals based on mixed Br^-/Cl^- perovskite layers, Suzuki et al. show, using solid-state NMR (Cl nucleus) technique, that most of Cl^- ions preferentially occupy the positions in the equatorial planes of layers.[18c] Coming back on the XRPD study, we suggest that the evolution of cell parameters along the transformation process (Figure 3), that is, notably the decrease of *a*- and *b*-axes contained in equatorial planes of perovskite layers, can correspond to an atomic reorganization in layers, leading to the presence of bromide in equatorial planes. By the way, we notice that the *a* and *b* parameters of the **B** phase (8.371 and 8.607 Å, respectively) are in the range of those usually observed for $PbBr_2$ planes of $PbBr_4$-based hybrid perovskites (from $a = 8.03$ Å, $b = 8.19$ Å[19] to $a = 8.46$ Å, $b = 8.64$ Å).[6d]

Conclusion

In summary, we described the organic−inorganic reaction under the solid state which produce the novel hybrid (Br-$(CH_2)_2$-$NH_3)_{2-x}$(I-$(CH_2)_2$-$NH_3)_x$$PbBr_xI_{4-x}$. This transformation has been followed by thermodiffractometry, and both solid state ^{13}C NMR and ESI/MS measurements have been adopted in the estimatiom of the rate of halide substitution. We showed that the first step of this reaction is the standing up of molecules, together with the substitution of (approximately) half organic bromine (A phase, composition of $x \approx 1$). Then, as the experiment time or the temperature increases, the substitution reaction continues (B phase, $x_{max} \approx 1.85$), and this is accompanied by an atomic reorganization in the mixed halide perovskite layers. Figure 6 summarizes the mechanism of the transformation, the final compound being ideally drawn with $PbBr_{2(eq)}I_{2(ap)}$ ($x = 2$) perovskite layers.

This unprecedented solid-state reaction between organic and inorganic components of a hybrid perovskite can be considered as a completely new strategy to achieve interesting hybrid perovskites.

Acknowledgment. We thank Pays de la Loire region for a post-doctoral fellowship to W.B.

Supporting Information Available: Crystallographic data, including the single crystal study of (X-$(CH_2)_2$-$NH_3)_2PbX_4$ (X = Br, I, A phase) and cell refinements of (Br-$(CH_2)_2$-$NH_3)_{2-x}$(I-$(CH_2)_2$-$NH_3)_x$$PbBr_xI_{4-x}$, thermal analysis (TGA, DSC), and details of the ^{13}C solid-state NMR and mass spectroscopy studies. This material is available free of charge via the Internet at http://pubs.acs.org.

IC070240G

(18) (a) Kitazawa, N. *Jpn J. Appl. Phys.* **1997**, *36*, 2272. (b) Kitazawa, N. *Mater. Sci. Eng.* **1997**, *B49*, 233. (c) Suzuki, Y.; Kubo, H. *J. Phys. Soc. Jpn.* **1983**, *52*, 1420. (d) Staulo, G.; Bellito, C. *J. Mater. Chem.* **1991**, *1*, 915−918.

(19) Corradi, A. B.; Ferrari, A. M.; Pellacani, G. C.; Saccani, A.; Sandrolini, F.; Sgarabotto, P. *Inorg. Chem.* **1999**, *38*, 716.